Analysis of the optical force in the Micro Ring Resonator

Avigdor Einat and Uriel Levy*

Department of Applied Physics, The Benin School of Engineering and Computer Science, The Center for Nanoscience and Nanotechnology, The Hebrew University of Jerusalem, Jerusalem, 91904, Israel
** ulevy@cc.huji.ac.il*

Abstract: We study the optical force in a micro ring resonator coupled to a bus waveguide, using the coupled mode theory and a numerical Finite Element Method. We show that the resonance enhancement of the force is diminished by the opposing contributions of the attractive and the repulsive forces related to the symmetric and the anti symmetric modes in the coupling region. We show that this limiting factor can be removed by adding asymmetry to the system, e.g. by modifying one of the waveguides. Furthermore, we study for the first time a combined system in which the micro ring resonator is coupled to a one dimensional photonic crystal waveguide. This modified geometry allows further enhancement of the optical force via the combination of optical resonances and slow light effect.

OCIS codes: (120.4880) Optomechanics; (130.3120) Integrated optics devices; (350.4238) Nanophotonics and photonic crystals.

References and links

1. D. Van Thourhout and J. Roels, "Optomechanical device actuation through the optical gradient force," Nat. Photonics **4**(4), 211–217 (2010).
2. J. Ng, C. T. Chan, P. Sheng, and Z. Lin, "Strong optical force induced by morphology-dependent resonances," Opt. Lett. **30**(15), 1956–1958 (2005).
3. M. L. Povinelli, S. G. Johnson, M. Loncar, M. Ibanescu, E. J. Smythe, F. Capasso, and J. D. Joannopoulos, "High-Q enhancement of attractive and repulsive optical forces between coupled whispering-gallery- mode resonators," Opt. Express **13**(20), 8286–8295 (2005).
4. M. L. Povinelli, M. Lončar, M. Ibanescu, E. J. Smythe, S. G. Johnson, F. Capasso, and J. D. Joannopoulos, "Evanescent-wave bonding between optical waveguides," Opt. Lett. **30**(22), 3042–3044 (2005).
5. A. Mizrahi and L. Schächter, "Mirror manipulation by attractive and repulsive forces of guided waves," Opt. Express **13**(24), 9804–9811 (2005).
6. A. Mizrahi and L. Schächter, "Two-slab all-optical spring," Opt. Lett. **32**(6), 692–694 (2007).
7. P. T. Rakich, M. A. Popovic, M. Soljacic, and E. P. Ippen, "Trapping, corralling and spectral bonding of optical resonances through optically induced potentials," Nat. Photonics **1**(11), 658–665 (2007).
8. F. Riboli, A. Recati, M. Antezza, and I. Carusotto, "Radiation induced force between two planar waveguides," Eur. Phys. J. D **46**(1), 157–164 (2008).
9. W. H. P. Pernice, M. Li, and H. X. Tang, "Theoretical investigation of the transverse optical force between a silicon nanowire waveguide and a substrate," Opt. Express **17**(3), 1806–1816 (2009).
10. W. H. P. Pernice, M. Li, K. Y. Fong, and H. X. Tang, "Modeling of the optical force between propagating lightwaves in parallel 3D waveguides," Opt. Express **17**(18), 16032–16037 (2009).
11. L. Zhu, "Frequency dependence of the optical force between two coupled waveguides," Opt. Lett. **34**(18), 2870–2872 (2009).
12. W. H. P. Pernice, M. Li, and H. X. Tang, "A mechanical kerr effect in deformable photonic media," Appl. Phys. Lett. **95**(12), 123507 (2009).
13. J. Ma and M. L. Povinelli, "Large tuning of birefringence in two strip silicon waveguides via optomechanical motion," Opt. Express **17**(20), 17818–17828 (2009).
14. P. T. Rakich, M. A. Popović, and Z. Wang, "General treatment of optical forces and potentials in mechanically variable photonic systems," Opt. Express **17**(20), 18116–18135 (2009).
15. A. Mizrahi, K. Ikeda, F. Bonomelli, V. Lomakin, and Y. Fainman, "Self-alignment and instability of waveguides induced by optical forces," Phys. Rev. A **80**(4), 041804 (2009).

#149949 - $15.00 USD Received 28 Jun 2011; revised 2 Sep 2011; accepted 5 Sep 2011; published 3 Oct 2011

16. V. Liu, M. Povinelli, and S. Fan, "Resonance-enhanced optical forces between coupled photonic crystal slabs," Opt. Express **17**(24), 21897–21909 (2009).
17. S. Huang and G. S. Agarwal, "reactive Coupling Induced Normal Mode Splittings in Microdisk Resonators Coupled to Waveguides," Phys. Rev. A **81**(5), 053810 (2010).
18. C. Huang and L. Zhu, "Enhanced optical forces in 2D hybrid and plasmonic waveguides," Opt. Lett. **35**(10), 1563–1565 (2010).
19. W. H. P. Pernice, M. Li, D. Garcia-Sanchez, and H. X. Tang, "Analysis of short range forces in opto-mechanical devices with a nanogap," Opt. Express **18**(12), 12615–12621 (2010).
20. J. Ma and M. L. Povinelli, "Effect of periodicity on optical forces between a one-dimensional periodic photonic crystal waveguide and an underlying substrate," Appl. Phys. Lett. **97**(15), 151102 (2010).
21. R. Zhao, P. Tassin, T. Koschny, and C. M. Soukoulis, "Optical forces in nanowire pairs and metamaterials," Opt. Express **18**(25), 25665–25676 (2010).
22. M. Li, W. H. P. Pernice, C. Xiong, T. Baehr-Jones, M. Hochberg, and H. X. Tang, "Harnessing optical forces in integrated photonic circuits," Nature **456**(7221), 480–484 (2008).
23. M. Li, W. H. P. Pernice, and H. X. Tang, "Tunable bipolar optical interactions between guided lightwaves," Nature Photonics **3**(8), 464–468 (2009).
24. J. Roels, I. De Vlaminck, L. Lagae, B. Maes, D. Van Thourhout, and R. Baets, "Tunable optical forces between nanophotonic waveguides," Nat. Nanotechnol. **4**(8), 510–513 (2009).
25. W. H. P. Pernice, M. Li, and H. X. Tang, "Optomechanical coupling in photonic crystal supported nanomechanical waveguides," Opt. Express **17**(15), 12424–12432 (2009).
26. J. Rosenberg, Q. Lin, and O. Painter, "Static and dynamic wavelength routing via the gradient optical force," Nature Photonics **3**(8), 478–483 (2009).
27. G. S. Wiederhecker, L. Chen, A. Gondarenko, and M. Lipson, "Controlling photonic structures using optical forces," Nature **462**(7273), 633–636 (2009).
28. G. S. Wiederhecker, S. Manipatruni, S. Lee, and M. Lipson, "Broadband tuning of optomechanical cavities," Opt. Express **19**(3), 2782–2790 (2011).
29. M. Eichenfield, C. P. Michael, R. Perahia, and O. Painter, "Actuation of micro-optomechanical systems via cavity-enhanced optical dipole forces," Nat. Photonics **1**(7), 416–422 (2007).
30. M. Li, W. H. P. Pernice, and H. X. Tang, "Reactive cavity optical force on microdisk-coupled nanomechanical beam waveguides," Phys. Rev. Lett. **103**(22), 223901 (2009).
31. J. Chan, M. Eichenfield, R. Camacho, and O. Painter, "Optical and mechanical design of a "zipper" photonic crystal optomechanical cavity," Opt. Express **17**(5), 3802–3817 (2009).
32. M. Eichenfield, R. Camacho, J. Chan, K. J. Vahala, and O. Painter, "A picogram- and nanometre-scale photonic-crystal optomechanical cavity," Nature **459**(7246), 550–555 (2009).
33. M. Eichenfield, J. Chan, R. M. Camacho, K. J. Vahala, and O. Painter, "Optomechanical crystals," Nature **462**(7269), 78–82 (2009).
34. Q. Lin, J. Rosenberg, D. Chang, R. Camacho, M. Eichenfield, K. J. Vahala, and O. Painter, "Coherent mixing of mechanical excitations in nano-optomechanical structures," Nature Photonics **4**(4), 236–242 (2010).
35. Y. G. Roh, T. Tanabe, A. Shinya, H. Taniyama, E. Kuramochi, S. Matsuo, T. Sato, and M. Notomi, "Strong optomechanical interaction in a bilayer photonic crystal," Phys. Rev. B **81**(12), 121101 (2010).
36. T. P. M. Alegre, R. Perahia, and O. Painter, "Optomechanical zipper cavity lasers: theoretical analysis of tuning range and stability," Opt. Express **18**(8), 7872–7885 (2010).
37. A. H. Safavi-Naeini, T. P. M. Alegre, M. Winger, and O. Painter, "Optomechanics in an ultrahigh-Q two-dimensional photonic crystal cavity," Appl. Phys. Lett. **97**(18), 181106 (2010).
38. J. D. Jackson, *"Classical Electrodynamics"*, 3rd ed. (Wiley, 1998), Chap. 6.7.
39. K. Okamoto, *"fundamentals of optical waveguides"*, 2nd ed. (Elsevier, 2006), Chap. 2.2.
40. H. Kogelnik, *"Topics in Applied Physics"* (Springer-Verlag, 1975), Vol. 7, Chap. 2.
41. D. Goldring, U. Levy, I. E. Dotan, A. Tsukernik, M. Oksman, I. Rubin, Y. David, and D. Mendlovic, "Experimental measurement of quality factor enhancement using slow light modes in one dimensional photonic crystal," Opt. Express **16**(8), 5585–5595 (2008).

1. Introduction

Optical forces (OF) are the subject of extensive research over the last few decades. Specifically, in recent years the OF has been explored in the context of nanophotonic devices. The advancement in nano fabrication capabilities, providing additional mechanical degrees of freedom, promoted the theoretical and the experimental efforts in this field of research. A comprehensive review describing the topic of optomechanical device actuation through the gradient optical force can be found in [1]. Several papers performed a theoretical study of the forces between waveguide (WG) structures in various configurations and investigated several potential applications [2–21]. The OF was measured and characterized experimentally in numerous WG configurations [22–25]. A recent effort is devoted to the

#149949 - $15.00 USD Received 28 Jun 2011; revised 2 Sep 2011; accepted 5 Sep 2011; published 3 Oct 2011

study of OF in photonic resonators, for two major reasons: 1 – The OF is resonantly enhanced via the mechanism of electromagnetic (EM) field enhancement at resonance. 2 - The narrow spectral line of photonic resonators allows substantial tuning of the optical transmission by applying OF. For example, transmission tuning via the enhancement of the OF was demonstrated using double ring structures [26–28] and micro disk resonators (MDR) [29,30]. Significant enhancement in OF and transmission tuning can be also obtained in Photonic crystals (PhC) systems by exploiting the dispersion of the band diagram and the slow light effect [31–37].

This manuscript begins by studying the opto-mechanical effect in the system of the Micro Ring Resonator (MRR). More specifically, we explore the force that acts on a free standing bus WG as a result of the circulating light in the resonator. Based on previous works, we use the coupled mode theory (CMT) to develop a new model which provides better understanding of the OF in the vicinity of the resonance. The model shows that as long as the bus WG and the MRR WG are identical, both the attractive (symmetric) and the repulsive (anti-symmetric) forces will be present at resonance, and thus the resonant enhancement of the OF will be diminished. Following this result, we numerically show that the force cancelation can be overcome by modifying one of the WGs, such that the relative phase between the two WGs at resonance can be controlled. Furthermore, we consider a novel configuration allowing further enhancement of the OF by the coupling of an MRR to a bus WG composed of a 1-D PhC. This modified geometry provides OF enhancement of about 35.

The paper is organized as follows: in section 2 we develop the analytical model for calculating the OF and present numerical simulations which validate the model and extend it to the a-symmetric case. In addition, we calculate the tuning of the transmission spectrum taking into account the mutual influence between the OF and the mechanical deflection of the free standing WG. In section 3 we study the effect of adding a periodic perturbation to the bus WG and show further enhancement of the OF as a result of the slow light effect. Section 4 concludes the paper.

2. The OF in the system of MRR coupled to a standard free standing strip WG

Our goal is to investigate the OF acting on the bus WG which is coupled to an MRR. Schematic description of the system is shown in Fig. 1.

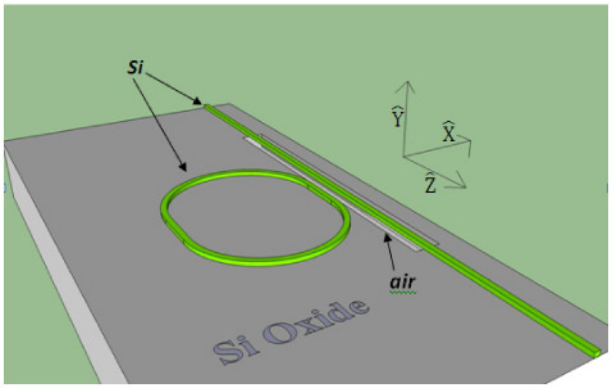

Fig. 1. Schematic diagram of the investigated structure. The system consists of an MRR coupled to a bus WG. The substrate under the bus WG is etched to create a free standing mechanical beam. For simplicity we perform a 2-D analysis but we keep the 3-D picture representation for visualization purposes.

2.1 Analytical approach

We begin by developing an analytical model based on the CMT approach allowing to calculate the OF. For simplicity, we consider a 2-D rather than a 3-D structure. While there

#149949 - $15.00 USD Received 28 Jun 2011; revised 2 Sep 2011; accepted 5 Sep 2011; published 3 Oct 2011

are significant differences in the force distribution between the 2-D and the 3-D structure, the 2-D analysis is sufficient for understanding the basic physics of the analyzed devices. Moreover, in some cases in can be used as a good approximation for 3-D structures, as briefly discussed towards the end of this manuscript. A schematic diagram showing our model is presented in Fig. 2a. To simplify the problem we consider a symmetric coupling region having its mirror symmetry in the middle of the coupling region, as shown in Fig. 2b. The system is excited by an EM wave of time-dependency $e^{i\omega t}$, and all the WGs are assumed to support a single mode.

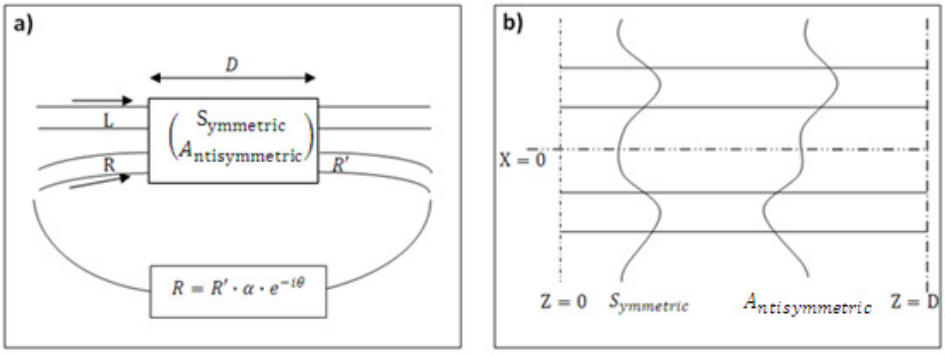

Fig. 2. Schematics of the 2-d system. (a) The notations of the EM fields in the bus WG and in the MRR as well as the phase accumulation in the MRR are shown. (b) The coupling region is sketched together with the two supermodes.

The time-averaged OF acting on the bus WG along the x-axis is calculated via Maxwell's stress tensor (MST) [38]. For our structure, it is given by (for Transverse electric –TE polarization) [5,8]:

$$F_x = \frac{1}{4}\cdot[-\varepsilon_0 \left|E_y\right|^2 + \mu_0(\left|H_x\right|^2 - \left|H_z\right|^2)] \tag{1}$$

We assume a coupling region in which the gap between the two WGs is constant. As a result, the geometry maintains its mirror symmetry which allows the decomposition of the incident EM field into symmetric (S) and anti-symmetric (A) modes. These are the eigenmodes of the coupling region.

Following previous work [10] one can express the incident field at the coupling region by

$$\psi = L + R \tag{2}$$

Where, ψ stands for the magnetic or electric field component, while L and R are the incident fields at each of the bus WGs. Generally, L and R can be arbitrarily chosen. However, in the case of an MRR, R is replaced by $R' = w \cdot R$ where R is identical to L both in its amplitude and its phase and w is the complex ratio between the field in the MRR and the incident field. For our structure, one can use CMT [39], to obtain:

$$w = \frac{-i\alpha \cdot e^{-i\theta}\sin(\kappa \cdot D)}{1-\alpha \cdot e^{-i\theta}\cos(\kappa \cdot D)} \tag{3}$$

Where, α and θ are the field amplitude fraction remaining after a roundtrip in the ring and the phase accumulated in the resonator roundtrip, respectively. D is the coupling region's length, and κ is the coupling coefficient between the WGs. Therefore, Eq. (2) takes the modified form of:

#149949 - $15.00 USD Received 28 Jun 2011; revised 2 Sep 2011; accepted 5 Sep 2011; published 3 Oct 2011

$$\psi = L + w \cdot R \tag{4}$$

At $z = 0$ we express the fields in each WG as a superposition of symmetric and anti-symmetric modes:

$$\begin{pmatrix} L \\ R \end{pmatrix} = \begin{pmatrix} a & b \\ c & d \end{pmatrix} \begin{pmatrix} S \\ A \end{pmatrix} \tag{5}$$

Where,

$$a = \int L \cdot S^* dx = \int R \cdot S^* dx = c, b = \int L \cdot A^* dx = -\int R \cdot A^* dx = -d \tag{6}$$

By substituting Eq. (4), (5) and (6) in Eq. (1), the OF acting on the bus WG can be written as:

$$\begin{aligned} F = {} & a^2 (1 + |w|^2 + 2\Re\{w\}) \cdot F_{sym} + b^2 (1 + |w|^2 - 2\Re\{w\}) \cdot F_{antisym} \\ & + 2ab\Re\{e^{-i \cdot \Delta\beta \cdot z} (1 - |w|^2 + 2i \cdot \Im\{w\})\} \cdot F_{\text{int}erference} \end{aligned} \tag{7}$$

Here, F_{sym} and $F_{antisym}$ are the OFs calculated for each of the two supermodes supported by two WGs system, $F_{\text{int}erference}$ is calculated by taking the product of the symmetric and the anti-symmetric field for every squared field component, $\Delta\beta = \beta_{symmetric} - \beta_{antisymmetric}$ is the difference between the propagation constants of the two supermodes, and z is the propagation length in the coupled region. Clearly, the third term oscillates with the propagation coordinate (z). For the purpose of calculating the OF acting on the WG we can simplify this term by taking its average value. This simplification is justified for large gaps between the WGs, where $\Delta\beta$ is relatively small. Moreover, for such a case it was shown [10] that the contribution from this beating term is negligible compared to the symmetric and anti-symmetric OF terms, because of the small overlap integral of the symmetric and anti-symmetric modes.

Figure 3 shows the OF as a function of wavelength as calculated from Eq. (7) for a specific 2-D MRR system, together with the MRR power enhancement spectrum.

#149949 - $15.00 USD Received 28 Jun 2011; revised 2 Sep 2011; accepted 5 Sep 2011; published 3 Oct 2011

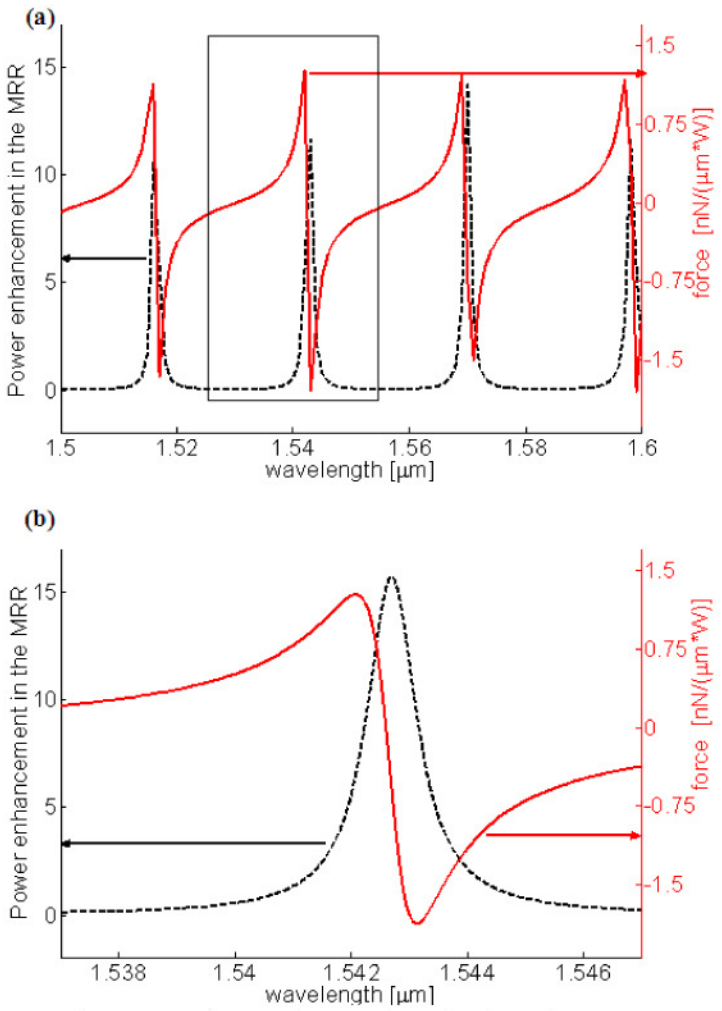

Fig. 3. (a) Power enhancement and OF as a function of wavelength. A 250nm gap is assumed between two 400nm slab WGs with $n = 2.446$. The WGs are coupled along a coupling region of $4\mu m$. The MRR properties are provided in the numerical section. (b) Zoom in on a specific resonance denoted by the rectangle.

From first glance, the results are surprising- the largest OF is not obtained at resonance, where the field enhancement is maximal, but rather at two extreme values, with opposing sign, occurring slightly before and after the resonance peak. These extreme values are indeed large compared to the force obtained in an equivalent two slabs system. However, the enhancement factor is in the order of 2-3, corresponding to the MRR power enhancement at these wavelengths which are slightly off resonance.

This counter-intuitive behavior of the force has been experimentally observed in a disk resonator system [30], and the results were explained by a quantum theoretical model. We next use our CMT-based model to explain this finding.

It has been shown [10] that the OF depends dramatically on the relative phase between the fields in two adjacent WGs. This relative phase controls the excitation of each of the eigenmodes in the system, and consequently the ratio between the attractive and repulsive components of the OF. In other words, the OF is not only a function of the fields' amplitudes but also a function of their relative phase.

#149949 - $15.00 USD Received 28 Jun 2011; revised 2 Sep 2011; accepted 5 Sep 2011; published 3 Oct 2011

We now go back to Eq. (7) and focus on the region of interest near resonance, where the amplitude of w tends towards its maximum. As appears from Eq. (3), at resonance one obtains $\Re(w)=0$, meaning that the relative phase between each component of the EM field in the bus WG and the MRR is $3\pi/2$. At typical gap separation, each of the coefficients of Eq. (6) approach the value of $1/2$, and thus at resonance Eq. (7) can be expressed as:

$$F\left|_{resonance}\cong\frac{1}{4}(1+\left|w\right|^2)\cdot[F_{sym}+F_{asym}]\right. \tag{8}$$

As was previously shown [4,5,8,23], at large enough separation gaps the symmetric force is attractive (negative sign in our conventions) whereas the anti-symmetric force is repulsive (positive sign). Thus, although the field enhancement is maximal, the opposing sign of the two force components will reduce the total net OF. On the other hand, if the relative phase tends towards 0 or π, while the system is still in the vicinity of resonance (in order to have a significant field in the MRR), maximal attractive or repulsive force will be obtained, respectively.

2.2 numerical simulations

While the analytical model supports the physical understanding of the parameters affecting the force in the system, it cannot be fully correlated to an actual structure. Therefore, numerical simulations are needed for quantitative design and analysis of the forces in the MRR system. Moreover, the numerical simulations allow coping with more complex structures, e.g. asymmetric structures. These will be shown to play an important role in our work. Throughout the paper, the numerical calculations are performed by the finite-element approach (COMSOL). We choose the basic strip WG to be made of silicon with cross sectional dimensions of $400nm\times300nm$ width and height respectively. These parameters were chosen after rigorous, 3-d MST calculations and are the result of a tradeoff between large forces that arise where the mode is not well confined [11] and the mode confinement needed for optimal operation of the MRR (e.g. controllable coupling and low bending loss). Furthermore, for the same reasons we consider only the less-confined polarization, in which the major electric field is polarized along the y-axis (TM- like polarization). In our 2-dimensional model, based on the Effective Index Method (EIM) [39,40], these parameters lead to an effective refractive index of $n_{eff}=2.52$ for silicon-on-SiO_2 WG.

We set the MRR radius to be $R=5.13\mu m$. We assume a racetrack structure, by adding two $2.67\mu m$ long straight WG sections to the MRR. First, we use the numerical simulation in order to validate the results of the analytical model. Indeed, the force obtained with the numerical calculation was very similar to that calculated by the analytical model. In Fig. 4 we present the electric field distribution in the coupling region at resonance and at adjacent wavelengths for which the force approaches its extreme values. As was predicted by the analytical model, the maximal repulsive (attractive) force is obtained when the relative phase between the fields in the WG and the MRR is close to π and 0, while at resonance the $3\pi/2$ phase difference at the beginning of the coupling region reduces the net force.

#149949 - $15.00 USD Received 28 Jun 2011; revised 2 Sep 2011; accepted 5 Sep 2011; published 3 Oct 2011

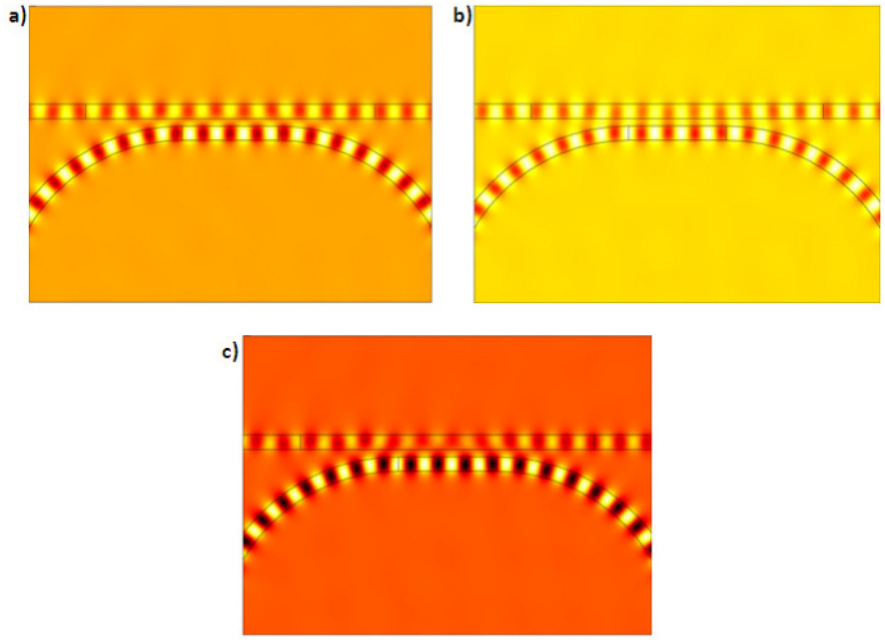

Fig. 4. The electric field distribution in the coupling region of the racetrack MRR is shown. Figure (a) [(b)] were calculated at wavelength in which the obtained force is maximal positive [negative], where the relative phase between the signals is close to π [0]. Figure (c) was calculated at a resonance wavelength in which the relative phase at the beginning of the coupling region is $3\pi/2$. The phase difference evolves and becomes $\pi/2$ at the output of the coupling region. For visualization purposes we modified the color scale between the 3 figures.

In order to maximize the OF, it is desired to operate at resonance, where the power enhancement is maximal. At the same time we wish to operate at phase matching condition, i.e. to have a relative phase approaching 0 or π, giving rise to the dominancy of either the symmetric or the anti-symmetric force term. To do so, we introduce an a-symmetry to the structure (by modifying the parameters of one of the WGs). From CMT it can be shown that in such a case the relative phase at resonance can deviate from $3\pi/2$, and in some cases it can even approach 0 or π.

The first step towards creating the needed asymmetry is by allowing the bus WG to be in a free standing configuration, whereas the MRR is assumed to be positioned on top of a SiO_2 substrate. This geometry supports the mechanical translation of the bus WG and at the same time is preferable for the obtaining of a stable MRR with high Q factor. In this configuration, the effective refractive index of the MRR and the bus WG are 2.52 and 2.446 respectively. However, from numerical calculations we conclude that this slight difference in effective indices is not sufficient, and the MRR's effective refractive index should be $n_{eff} = 2.66$, i.e. effective index difference of nearly 0.22. This can be achieved e.g. by increasing the height of the MRR from 300nm to 325nm. Alternatively, we can choose a wider MRR WG. For partial purposes the latter option is preferable because it does not require multi etching steps.

We repeat the numerical simulations with an MRR effective index value of 2.66. The obtained power enhancement and force as a function of wavelength in the vicinity of a single resonance are presented in Fig. 5, where the force and the power enhancement curves are

#149949 - $15.00 USD Received 28 Jun 2011; revised 2 Sep 2011; accepted 5 Sep 2011; published 3 Oct 2011

nearly consolidating, and the force obtains its maximum absolute value around the wavelength of resonance, where the power enhancement is maximal.

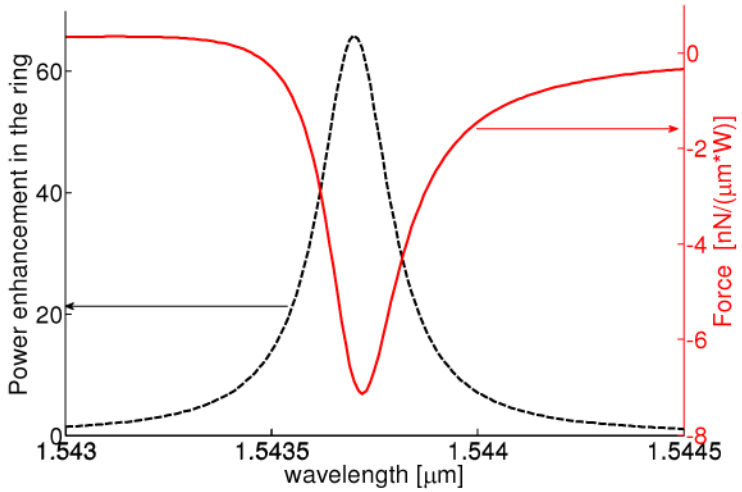

Fig. 5. The force in an asymmetric MRR system as a function of the wavelength. The effective refractive index of the MRR is assumed to be 2.66. The separation gap is 250nm. These parameters corresponds to quality factor of $Q \cong 10,000$.

With this improvement we can now investigate the obtained force values and their relation to the MRR power enhancement. In Fig. 6 we sketch the force as a function of wavelength for numerous separation gaps between the MRR and the bus WG. First, we notice the narrowing of the force curve as the gap separation increases. This is expected because the coupling between the bus WG and the MRR is decreasing, effectively increasing the Q factor of the MRR. The narrow force curve will be used in the next section, where we discuss the tunability of the optical system using optical forces. In addition, we notice an increase in the force at resonance with the decrease in the gap separation. Here we need to take into account two phenomena having opposite effect on the force. On one hand, by reducing the separation between two WGs, one expects the force to increase as a result of stronger interaction. On the other hand, the resonant enhancement of the force becomes less prominent, due to the decrease in Q factor. We now focus on this later effect by comparing the force at resonance to the force obtained in a double WG system with the same separation gap. The result is shown in the inset of Fig. 6. Indeed, we notice an increase in the force enhancement, following the improvement in the Q factor of the MRR. However, this enhancement does not follow the power enhancement in the MRR. This feature can be explained by the fact that the power is only enhanced in the MRR, but not in the bus WG.

#149949 - $15.00 USD Received 28 Jun 2011; revised 2 Sep 2011; accepted 5 Sep 2011; published 3 Oct 2011

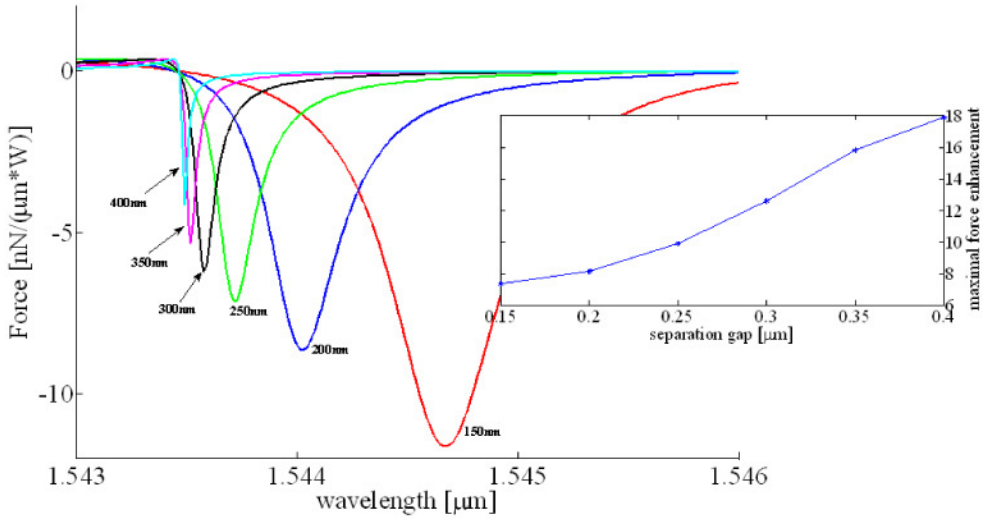

Fig. 6. Force as a function of wavelength for different gaps between the bus and the MRR. As can be seen, the Q factor grows with the increase of the separation gap. However, the magnitude of the force decreases with the increase in separation gap, because of the lower overlap between the mode and the WG. The inset shows the maximal force values normalized by the force that is obtained in the 2 slabs system for the same gap, as a function of the separation gap.

2.3 The mechanical response

In order to estimate the coupled opto-mechanical effect, we combine the EM simulations together with structural simulations to predict the motion of the bus WG as a result of the OF. We assume a separation gap of 250nm, for which the obtained quality factor and maximal force are $Q \cong 10,000$ and $\left|F_{\max}\right| \cong 7[nN/(\mu m \cdot W)]$ respectively (see Fig. 5). We assume the section of the air bridged WG, i.e. the free standing beam to be $28\mu m$ long. As an example, if we decouple the EM and the mechanical simulations, these parameters will result in maximal beam deflection of 5.6nm for an incident power of 50mW in the bus WG.

While the latter value provides an estimate for the strength of the effect, a more rigorous analysis which takes into account the mutual effect of the EM fields and the geometry of the device is needed. For example, a shift in the device geometry may result in a transition of the MRR out of resonance. This in turn will reduce the strength of the EM field in the resonator. As a consequence, the beam will tend towards its original geometry, and the process will repeat itself.

In Fig. 7 we show explicitly the combined opto-mechanical effect. We compare between low power (1mW) and higher power (25mW) feeding of the device. For the latter, the wavelength of maximum power in the MRR is blue shifted by about 1nm primarily due to the resonator's effective index's change in the coupling region resulting from the change in dimensions.

#149949 - $15.00 USD Received 28 Jun 2011; revised 2 Sep 2011; accepted 5 Sep 2011; published 3 Oct 2011

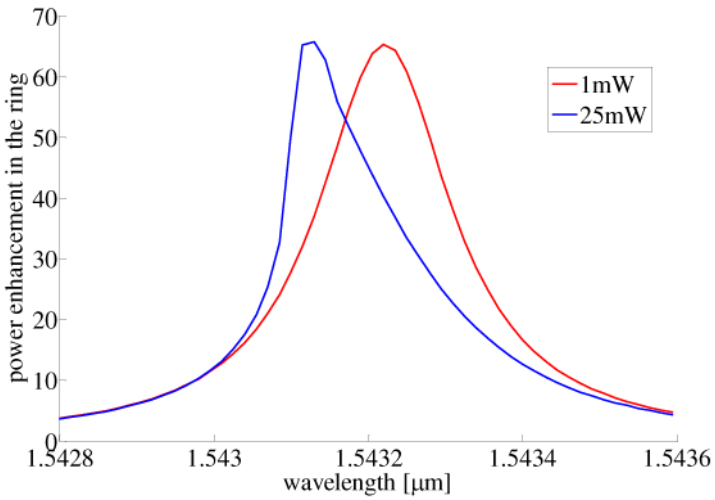

Fig. 7. Tuning the MRR using the optomechanical effect. The power enhancement in the resonator near resonance is shown for the suggested device, at two power levels in the WG.

3. The photonic-crystal-embedded MRR structure

In the previous sections we demonstrated the enhancement of the OF by the use of an MRR, combined with optimal selection of the phase shift between the light propagating in the MRR and in the bus WG. However, the force enhancement is still moderate, and consequently its effect on the optical signal propagating through the MRR is relatively small. This is because the enhancement is limited to the MRR, while the forces are obtained by the combined effect of the fields in both the MRR and the bus WG.

In order to further enhance the OF and increase its effect on the optical signal propagating in the structure, we next consider taking advantage of the slow light effect by adding a periodic perturbation to the bus WG. Specifically, we aim to operate in the vicinity of the band edge of the periodic structure, where the light experiences high group index. Simultaneously the parameters are chosen such that we operate at one of the resonances of the MRR.

The idea of utilizing the effect of slow light at the band edge to enhance optical forces has been recently utilized for enhancing the force between a free standing 1-D PhC bar and its underlying substrate [20]. Here we apply this concept for the first time in combination with the MRR structure for enhancing the OF.

We choose our periodic perturbation to be consisted of air holes that are fully etched into the Si WG. For hole diameter of 300 nm and periodicity of 415 nm we found the first band edge to be around the telecom wavelength of $\lambda = 1.55\mu m$. The group index at each optical frequency is calculated from the dispersion diagram using

$$n_g = c \cdot (\frac{\partial \omega}{\partial k})^{-1} \tag{9}$$

The force is expected to increase with the group index enhancement, i.e. the obtained group index normalized by the group index of an unperturbed WG (~4 for the Si WG).

We now validate the relation between the force enhancement and the slow light by calculating the OF in a structure of 2 perturbed WGs with respect to a structure of 2 unperturbed WGs. The double PhC WG structure exhibits a splitting in its dispersion diagram, corresponding to the symmetric and the anti-symmetric modes. Fig. 8a shows the group index as a function of wavelength for the single PhC WG and the double PhC WG,

#149949 - $15.00 USD Received 28 Jun 2011; revised 2 Sep 2011; accepted 5 Sep 2011; published 3 Oct 2011

together with the corresponding mode profiles. Fig. 8b shows the force enhancement (relatively to the equivalent unperturbed structure) obtained by MST calculation.

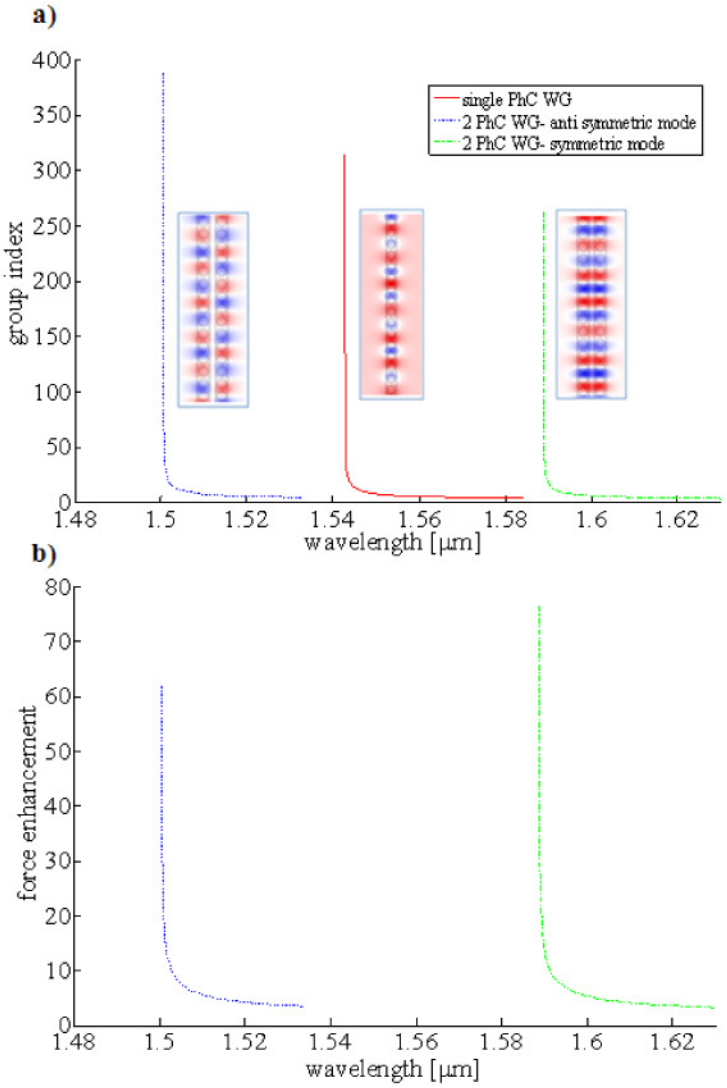

Fig. 8. (a) The group index in the vicinity of the first band edge of the PhC WG as a function of wavelength. Two structures are considered as shown in the insets with the electric field mode superimposed: A single silicon WG with periodic perturbation of air holes (data can be found in the paper) and two coupled silicon WGs with periodic perturbation of holes. (b) The force obtained in the periodically perturbed double WG system, normalized by the value obtained in the equivalent unperturbed structure.

As expected, the force is significantly enhanced as the wavelength approaches the band edge, and the enhancement factor is close to the enhancement of the group index. The slight discrepancy between the group index enhancement and the force enhancement may be attributed to variation in mode profile as the wavelength approaches the band edge, as well as to numerical inaccuracies in the proximity of the band edge, in particular in estimating the group index near the band edge.

After validating that the periodic perturbation enhances the OF, we simulate the desired structure, consisting of a bus WG with 30 holes (with similar parameters as in the previous

#149949 - $15.00 USD Received 28 Jun 2011; revised 2 Sep 2011; accepted 5 Sep 2011; published 3 Oct 2011

example) drilled into it. This bus WG is coupled to an MRR, as shown in Fig. 9a. The separation gap is 250 nm. This structure gives rise to the coupling between two resonators. The first resonator is the 1-D PhC WG, with the interfaces between its Bloch mode and the mode of the ridge WG serving as mirrors. Such structures were previously shown to be useful in enhancing the quality factor as a result of the high group index towards the band edge [41]. The other resonator is the MRR. Clearly, the goal is to match the resonance frequencies of these two resonators. To do so, we tune the effective refractive index of the MRR. As mentioned previously, this can be achieved e.g. by modifying the height or the width of the MRR WG. The transmission spectrum near the band edge is shown in Fig. 9b as a function of the wavelength and the MRR refractive index.

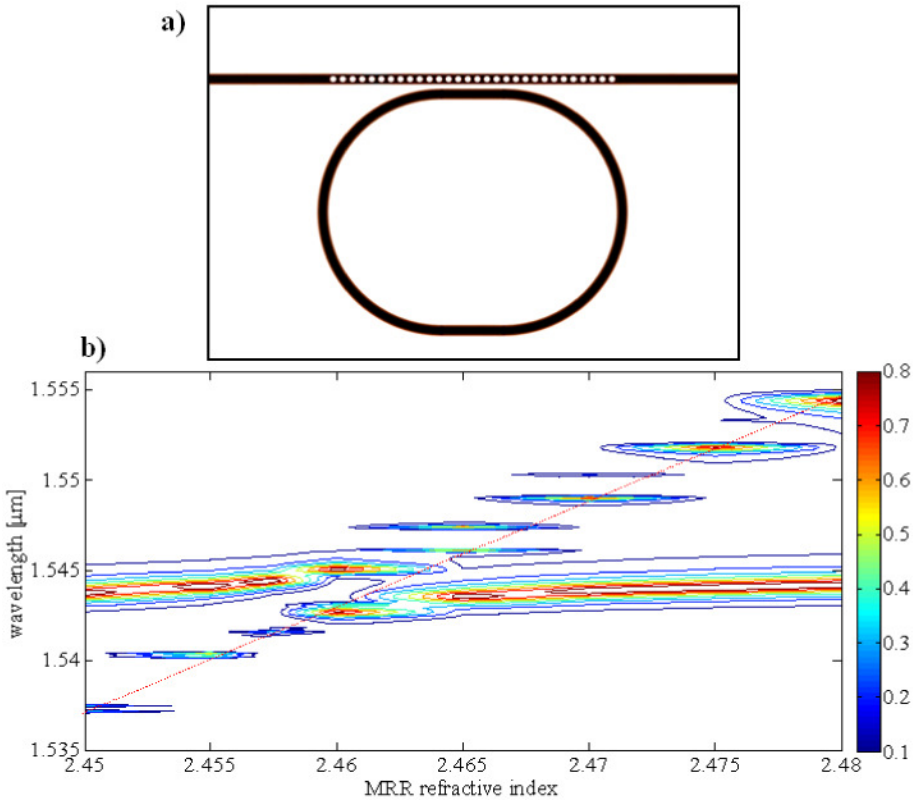

Fig. 9. (a) drawing of the simulated structure, consisting of an MRR separated from a bus WG. Periodic perturbation of 30 air holes is embedded into the WG. The specific parameters are given in the text. (b) Transmission of light emerging from the structure of the MRR and a periodically perturbed bus WG as a function of the incident wavelength and the MRR refractive index. Red dotted line represents the shift in resonance wavelength as a function of variations in the MRR refractive index.

By observing Fig. 9b we can identify the two resonances. First, we notice a resonance close to $\lambda = 1.545 \mu m$ which is almost not affected by the change in the MRR refractive index. Therefore, this resonance is attributed to the 1-D PhC resonator. Additionally, we identify another transmission peak, with its resonance wavelength depends linearly on the MRR refractive index. This transmission peak is due to the MRR resonance. At the intersection point (around $n_{MRR} = 2.46$) between the two resonances, a resonances splitting is obtained.

Naively, one would expect a maximal OF value to be obtained where the PhC and the MRR experience resonance simultaneously. However, our simulations show that the

#149949 - $15.00 USD Received 28 Jun 2011; revised 2 Sep 2011; accepted 5 Sep 2011; published 3 Oct 2011

maximal OF value is obtained slightly below the intersection point, at $n_{MRR} = 2.4572$. This fact may be understood as a trade-off between the resonances intersection on one hand and group index enhancement on the other hand.

The force and the transmission as a function of the wavelength for this optimal value are shown in Fig. 10. As shown we obtain a maximal force of $\sim 25[nN/(\mu m \cdot W)]$ implying an enhancement of ~35 compared with the 2 unperturbed WGs system.

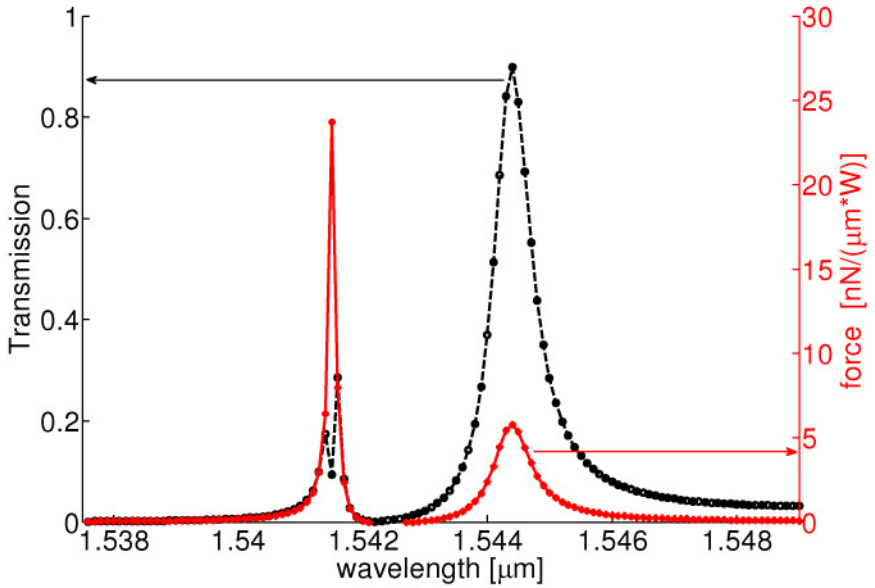

Fig. 10. The transmission and the force acting on the WG, plotted against the wavelength in the region next to the band edge. The refractive index of the MRR WG is assumed to be $n_{MRR} = 2.4572$.

The manuscript is focused on 2-D geometry which is different from the full 3-D description of actual structures. However, in some cases the 2-D analysis can provide results which can be considered as a good approximation of the results that would be obtained in the 3-D structure by the use of the Effective Index Method (EIM). As an example, we use the system of two optical WGs and compared the obtained force in two cases: full 3-dimensional system and an approximated system based on the EIM (effective index method). We first considered a structure of two Si WGs each having cross sectional dimensions of $400nm \times 300nm$, and separated along the horizontal direction. In Fig. 11 the calculated OF component is plotted against the separation gap (blue lines) for the out of plane polarization (major electric field is polarized along the y-axis). Next, we calculated the OF for the same system using the effective index approach, where the y- dimension was eliminated, by replacing the air-300 nm silicon-air structure with a single infinite layer having an effective refractive index of 2.446. The calculated forces are also plotted in Fig. 11 (red lines).

#149949 - $15.00 USD Received 28 Jun 2011; revised 2 Sep 2011; accepted 5 Sep 2011; published 3 Oct 2011

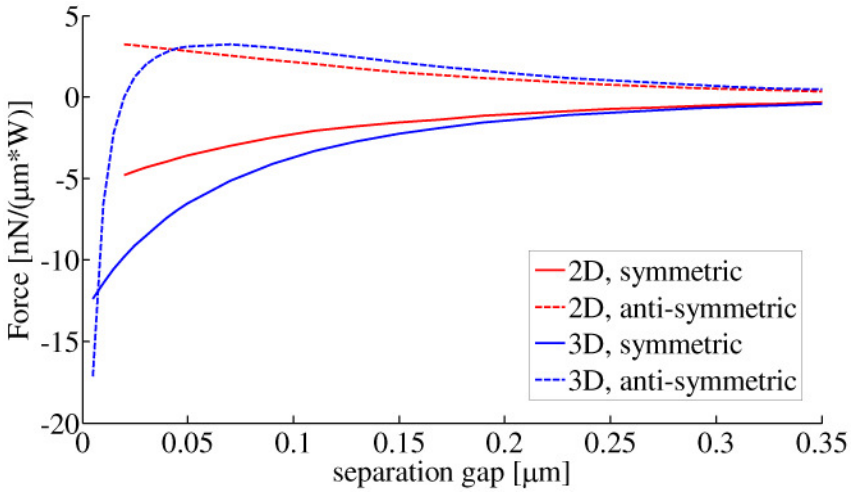

Fig. 11. The OF calculated for two Si (n = 3.45) WGs having identical cross sections of $400nm \times 300nm$. The WGs are excited by an out of plane (TM) polarized, laser source at the wavelength of $\lambda = 1.55\mu m$. The broken lines (solid lines) represent the force for an anti-symmetric (symmetric) mode excitation. The blue lines are the full three dimensional calculation, while the red lines refer to a two dimensional system, effectively two slabs of $400nm$ with n = 2.446.

As can be seen, the OFs obtained for the 3-D and the 2-D geometries are very similar, as long as the gap between the WGs exceeds approx. 200 nm. As was discussed, our MRR have a racetrack shape and thus a relatively large gap is needed in order to keep the coupling between the WG and the MRR low. Therefore, we can qualitatively use the 2-D model for our calculations. Yet, one should keep in mind that the actual resonance frequencies and the quality factors may be slightly different in real (3-D) geometry, and thus the obtained results are qualitative.

4. Conclusions

We analyzed the OF acting on a bus WG coupled to a MRR, using the CMT and a numerical Finite Element Method. Our analytical model shows that the resonance enhancement of the force as a result of the MRR's power enhancement is diminished by the opposing contributions of the attractive and the repulsive forces related to the symmetric and the anti-symmetric modes in the coupling region. We suggested that adding asymmetry to the system by changing one of the WGs removes this restriction. We further proposed adding periodic perturbation to the bus WG in order to create a one dimensional PhC WG, and operating at the slow light regime. By this procedure and by careful matching between the MRR and the PhC resonances, this modified geometry allows further enhancement of the OF via the combination of optical resonances and slow light effect.

Acknowledgements

The authors thank Raviv Yitzhaki, Boris Desiatov, and Ilya Goykhman for fruitful discussions and acknowledge the funding of the Israeli Science Foundation.

#149949 - $15.00 USD Received 28 Jun 2011; revised 2 Sep 2011; accepted 5 Sep 2011; published 3 Oct 2011